Synchronization with DMT Modulation

Thierry Pollet and Miguel Peeters, Alcatel

ABSTRACT In a digital transmission system, synchronization is an essential receiver function. Accurate timing information must be known to the demodulator in order to produce reliable estimates of the transmitted data sequence. In this article, synchronization for discrete multitone transmission is examined. The effect of imperfect timing on the receiver performance is investigated. An overview of timing estimation and correction circuits based on data-aided and non-data-aided algorithms derived from maximum-likelihood estimation theory is given.

In digital data communications, binary information is converted by means of a modulator into a continuous-time signal which is sent over the transmission channel. A digital receiver is to extract the information sequence from a discrete-time signal obtained after sampling and quantizing the distorted signal presented to the demodulator. At the receiver, accurate timing recovery is critical to obtain performance close to that of the optimal receiver. Growing out of classical estimation theory [1], synchronization has evolved into an autonomous research area that has been studied in depth over the last decades [2–5]. Many synchronizer algorithms can be related to the maximum likelihood (ML) criterion. According to this criterion, the estimates of the timing parameters maximize the likelihood function. The likelihood function depends on the considered modulation format — such as single-carrier quadrature amplitude modulation (QAM), vestigial sideband (VSB), or discrete multitone transmission (DMT) — the characteristics of the transmission channel, and the statistical properties of the noise added to the signal. Ad hoc synchronizers, which are not related to the ML criterion, exploit obvious properties of the transmitted (cyclo-stationary) signal. Usually, the incoming signal is passed through a nonlinearity. This gives rise to spectral lines which are used to extract the symbol timing [6].

Two types of synchronizer structures can be distinguished; data-aided (DA) synchronizers use the receiver's decisions (decision-directed) or a training sequence in computing the timing estimates. Non-data-aided (NDA) structures operate independent of the transmitted information sequence. The timing estimates maximize the NDA likelihood function, which is obtained by averaging the likelihood function over the random information variables.

In this article the emphasis is on DA and NDA synchronizer structures for DMT modulation suitable for digital implementation. Transmission over time-invariant dispersive channels is considered. The presented structures are used in asynchronous digital subscriber line (ADSL) and very-high-rate DSL (VDSL) DMT-based transceivers for high-rate data transmission over twisted pair copper wire.

Discrete Multitone Modulation

DMT is a line code standardized for high-rate transmission over copper telephony wires [7]. An excellent tutorial on DMT is given in [8]. The DMT transceiver (Fig. 1) splits the available bandwidth into a large number of subbands. In each subband a QAM-modulated carrier is transmitted. Modulation is performed digitally by means of an inverse fast Fourier transform (IFFT). If the DMT signal contains N carriers (see Table 1 for a glossary of all equation notation), the discrete-time signal can be obtained from a $2N$-point IFFT. Denote a_m^k the constellation point that modulates the kth carrier during the mth DMT symbol. The samples s_m^n at the IFFT output can be expressed as $s_m^n = \sum_{k=0}^{2N-1} a_m^k \exp(j(2\pi kn)/(2N))$. In order to generate a real signal the symbols fed to the IFFT must satisfy $(a_m^k)^* = a_m^{2N-k}$, $n \in [0, 2N-1]$. A circular prefix is appended to guarantee orthogonal signals at the receiver. The purpose is to simplify equalization of the dispersive channel. The samples are sent to a digital-to-analog (D/A) converter at the rate f_s. The transmit filter $p(t)$ removes the spectral repetitions of the discrete-time signal.

The demodulator samples the received signal $r(t)$ at the rate $\hat{f}_s$. In order to detect the transmitted symbols, the receiver processes blocks of $2N + \nu$ consecutive samples, from which the first ν samples are removed. An FFT is performed on the remaining samples. Assuming the composite channel response is

Glossary of Notation

N:	Number of tones in the DMT signal.
$2N$:	Size of IFFT to generate the discrete-time DMT signal.
a_m^k:	QAM symbol modulating the kth carrier during the mth DMT symbol period.
ν:	Length of guardband expressed in samples.
$s(t)$:	Continuous-time DMT signal at the transmitter.
$r(t)$:	Continuous-time DMT signal at the receiver.
T:	Sample period at the transmitter
D_m^n:	Difference between the time instant (normalized wrt. T) generated by the receiver Xtal and the desired time instant. m and n refer to the mth received symbol and nth sample from that symbol, respectively.
$\hat{D}_m^n$:	Estimate of D_m^n.
e_m^n, $\hat{e}_m^n$:	Timing error for the nth sample of the mth DMT symbol and its estimate.
$\hat{e}_m$:	TED output at the mth DMT symbol period.
Note:	when variables appear without subscript or superscript, they are independent of the DMT symbol period and sample instant, respectively.
SNR_k:	Signal-to-noise ratio at the kth tone.
f_s, $\hat{f}_s$:	Sample rate at the transmitter and receiver.
$\mathbf{h}(\varepsilon)$:	$(h_0(\varepsilon),\ldots,h_{2N-1}(\varepsilon))$ channel impulse response, with L nonzero values and receiver sampling phase ε.
$\mathbf{H}(\varepsilon)$:	$(H_0(\varepsilon),\ldots,H_{2N-1}(\varepsilon))$, channel transfer function.

0163-6804/99/$10.00 © 1999 IEEE

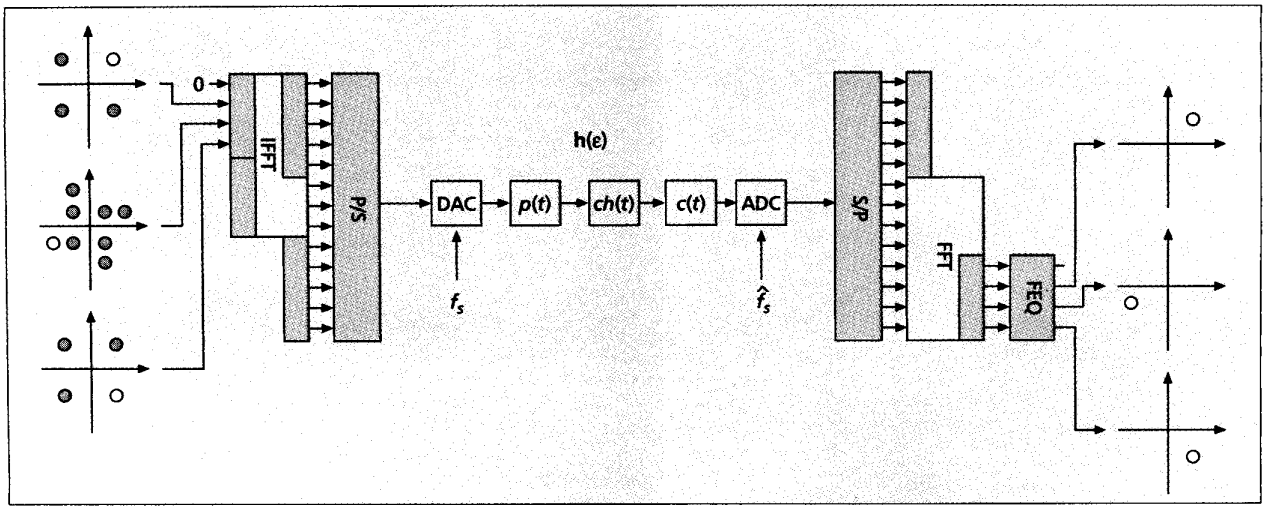

■ **Figure 1.** *A DMT transceiver.*

shorter than the guard time duration, channel equalization is performed by multiplying the FFT outputs with a single complex tap (FEQ). For each FFT output, the coefficient equals the inverse of the channel transfer function at the corresponding carrier frequency.

Synchronization in DMT Systems

Figure 2 depicts generic structures of a feed-back synchronizer. Essentially, the circuit consists of a timing error detector (TED) and timing adjustment unit (timing error corrector, TEC). Timing correction can be performed in the discrete-time (Fig. 2a) or continuous-time domain (Fig. 2b). In the continuous-time domain, timing adjustment can be performed by controlling the sampling phase. A filtered version of the TED output is fed to the device that determines the sampling instants (e.g., a voltage-controlled crystal oscillator, VCXO). In the digital domain, timing adjustment can be achieved by digital signal processing. In the sequel, the focus is on digital TEDs and timing correction that exploit the properties of the DMT signal.

Let us assume the composite transmission channel is distortionless and introduces a delay equal to DT. Hence, $h(t) = \delta(t - DT)$. The receiver estimates D (assume for now that this estimate is perfect) and splits the delay into an integer part Δ and its fractional part ε. Synchronization is performed as follows: the timing unit adjusts the sampling clock phase over εT. In addition, the symbol clock is delayed by skipping Δ samples. Therefore, in DMT transmission, two types of synchronization can be distinguished: *sample synchronization* and *symbol synchronization*. The sample synchronization unit guarantees frequency alignment of the receiver sampling clock with the transmitter sampling clock. It measures the fractional delay ε and corrects the sample timing accordingly. The *symbol clock synchronizer* unit detects, from the received sample sequence, the $2N + \nu$ samples that belong to the same received symbol and controls which samples are fed to the FFT.

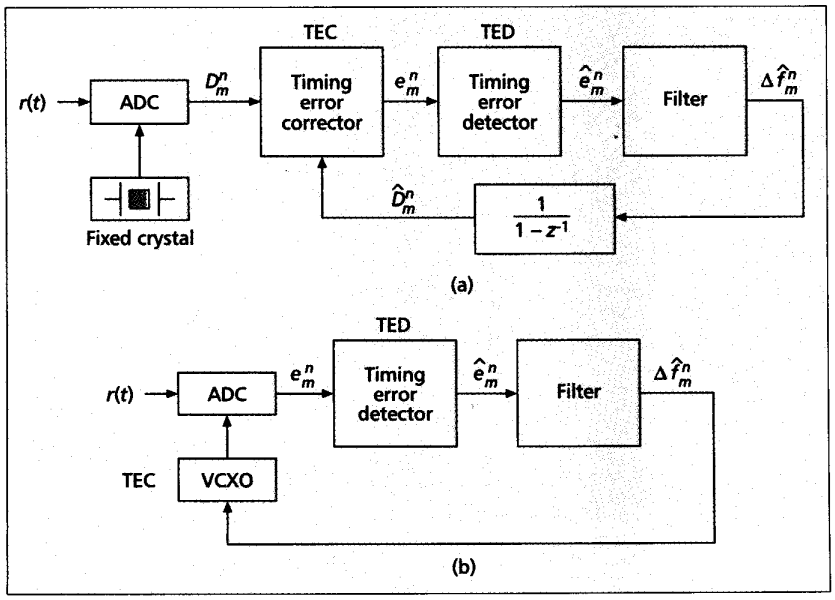

■ **Figure 2.** *Generic structures of a feedback synchronizer circuit: a) discrete-time correction; b) continuous-time correction.*

The Effect of a Transmission Delay

Figure 3 illustrates the transmission of a four-carrier DMT signal[1] over a channel $h(t)$. A guardband of five samples has been inserted ($\nu = 5$). By construction, the composite im0pulse response of the channel $h(t) = p(t) * ch(t) * c(t)$ is nonzero in a time interval which is shorter than the guardband. In this example, the impulse response is nonzero for $2T < t \leq 6T$. The discrete-time equivalent of the channel when sampling with phase ε is denoted by $\mathbf{h}(\varepsilon)$. The ideal symbol synchronizer will delay the receiver symbol clock over two samples ($\Delta = 2$) with respect to the transmitter symbol clock. The kth output of the FFT can now be expressed as $a_k^m H_k(\varepsilon)$ where $\mathbf{H}(\varepsilon)$ is the

[1] *The carriers at DC and Nyquist are not modulated.*

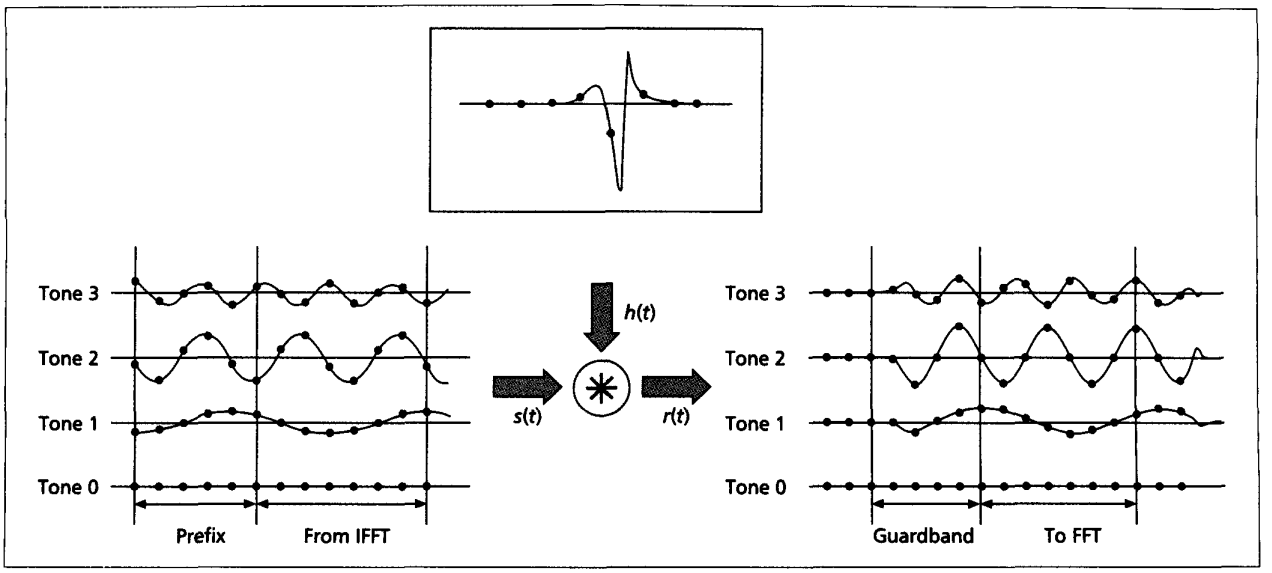

■ **Figure 3.** *Symbol alignment.*

FFT of $\mathbf{h}(\varepsilon + \Delta)$. This is because the part of the received continuous-time signal from which samples are sent to the FFT can be expressed as a sum of sinusoids with frequencies $(kf_s)/(2N)$.

The effect of a sample phase shift, $0 \leq \varepsilon < 1$, results in a rotation of the FFT outputs (i.e., $a_k^m H_k(\varepsilon) = a_k^m H_k(0)\exp(j(2\pi k\varepsilon)/(2N))$. Figure 4 depicts the effect of a sample phase shift over half a sample period (i.e., $\varepsilon = 0.5$). This shows that a sample phase shift can be compensated in the digital domain by rotating each FFT output over an angle proportional to the carrier index k and the phase shift ε. The above is correct as long as the sample phase shift is smaller than the difference between the channel impulse length and the guard time duration. This time domain shift ⇔ frequency domain rotation relation of the DMT signal is important in the design of the timing correction unit. In the sequel, this relationship will be referred to as the *delay-rotor* property. It is important to note that when the composite channel response transfer function has a (one-sided) bandwidth, B, larger than $1/(2T)$, the delay-rotor property is not valid for the carriers with carrier indices n satisfying $2N(1 - BT) < n < N$.

The choice of any symbol delay value other than two will result in intersymbol interference (ISI). Moreover, the orthogonality of the constituent signals of the DMT signal sent to the FFT is destroyed. The output of the FFT is distorted by intercarrier interference (ICI). ICI is a perturbation of the useful signal at the output of the FFT which consists of additive contributions that are proportional with symbols transmitted on carriers other than the considered carrier. The structure of ICI and ISI has been studied in [9].

NDA Symbol Timing Estimation and Correction

In [10], an NDA ML-based estimation of D has been derived for transmission over an additive white Gaussian channel. It is shown, that for low SNR values at the receiver, the logarithm of the NDA likelihood function, $L(D)$ (called the *log likelihood function*), can be approximated by

$$L(D) \approx L(\Delta,\varepsilon) = \sum_m \sum_{n=0}^{\nu-1} r((n+m(2N+\nu)+D)T) \times r^*((n+m(2N+\nu)+2N+D)T)$$

The receiver delays its symbol clock and sample clock phase over the values of Δ, ε that maximize $L(\Delta, \varepsilon)$. Essentially, the algorithm correlates the received sample sequence with a shifted version (over $2N$ samples) of that sequence. The maximum indicates the symbol boundaries. Because of the properties of the DMT signal, the computation can be simplified. Figure 5 depicts how $L(\Delta, \varepsilon)$ can be computed at the receiver: for a fixed sample timing phase ε, the circuit produces $L(\Delta, \varepsilon)$ for different values of D. The value of Δ which maximizes $L(\Delta, \varepsilon)$ results in an estimate of D with a maximal estimation

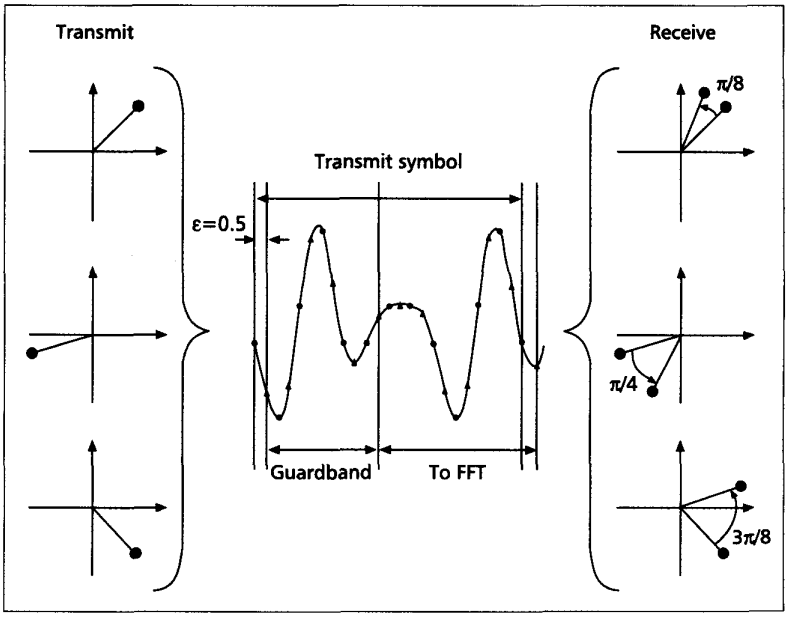

■ **Figure 4.** *The effect of a sample phase shift.*

error equal to half a sample period. Hence, to find the optimum timing according to the NDA ML criterion, an extensive search over ε, $-0.5 < \varepsilon < 0.5$, must be performed by adjusting the sampling phase of the sampling device. Alternatively, the delay ε can be realized in the digital domain by using interpolation techniques. Whereas for transmission over a dispersive channel, theoretically, a modified log likelihood function should be considered, the method developed for the ideal channel works well.

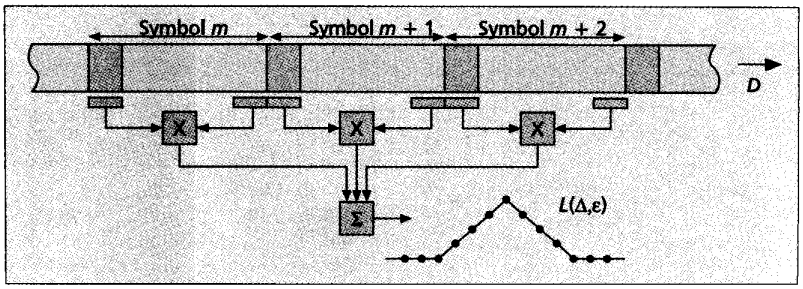

■ **Figure 5.** *NDA symbol timing estimation.*

Call $\hat{D}$ the estimate of D. When the residual timing error $(D - \hat{D})$ is smaller than the difference between the guard time and the channel impulse duration $(D - \hat{D} < \nu - L)$, correction of sample phase can be performed in the digital domain by rotating the FFT outputs. Adjustment of the sample phase of the sampling device or digital interpolation can hereby be avoided. However, a phase rotation introduced by the channel transfer function and a timing error both result in a rotation of the FFT outputs. As a consequence, the channel phase and timing error cannot be estimated separately. Therefore, the proposed synchronizer is essentially used for timing acquisition. The purpose is to reduce the initial timing error to a value smaller than half a sample period.

Ad Hoc Symbol Timing Estimation and Correction

Usually, the channel impulse response is longer than the guardband. Increase of the guardband is an inefficient method of avoiding ISI and ICI. Channel equalization is an alternative to eliminate interference. In time domain equalization [11], a digital linear filter is added at the receiver. The coefficients of the filter are computed such that the cascade of the composite channel and the filter yields an impulse response shorter than the guardband. In practice, the shortened impulse amplitude is very small outside the guardband, but nonzero (unless a zero forcing criterion is applied), creating residual ICI and ISI. Hence, the SNR on each carrier and capacity depend on the sampling instant. The *ideal* synchronizer circuit is the circuit that determines the timing such that a maximal capacity is obtained. It can easily be shown that this criterion is not necessarily equivalent to the ML criterion approach. Unfortunately, the *maximum capacity* criterion does not result in simple, low-complexity TEDs. This motivates the search for ad hoc synchronizer algorithms. One possible approach is to compute the timing D in such a way that the average ICI plus ISI power[2] is minimal. Assuming that all carriers in the multicarrier systems carry data, the average interference power, $V(D)$, is proportional to

$$V(D) \propto \sum_{n=-\infty}^{+\infty} w(n)h^2((n+D)T)$$

$$= \sum_{n=-\infty}^{+\infty} w(n-\Delta)h^2((n+\varepsilon)T)$$

where $w(n)$ is a window, as depicted in Fig. 6.

In a low-complexity implementation, the window can be replaced by a brick-wall window (nonzero only for ν values). Hence, finding the symbol timing is equivalent to searching for the maximal energy of the impulse response in a window limited to $\nu+1$ samples.

[2] *Here, average refers to taking the arithmetical average of the interference powers.*

Observe that this synchronization scheme requires the knowledge of the sampled composite impulse response. The impulse response can be measured at initialization of the modem, during which N sinusoids at the frequencies $(kf_s)/(2N)$ are transmitted. This can easily be realized with the DMT system by always transmitting the same DMT symbol during initialization and generating the multicarrier signal without guardband insertion. At the receiver, an FFT is performed and the outputs are corrected to remove the QAM modulation. Finally, an IFFT on the corrected signal yields a noisy estimate of the channel impulse response. The NDA ML method is very similar to the ad hoc structure which minimizes the average ICI plus ISI power. In the absence of noise, $E[L(D)]$ reduces to $V(D)$ where $w(n)$ is a triangular window with a duration of $2\nu + 1$ sample periods. Note that other ad hoc methods can be considered, for example, estimation of the timing based on a measurement of the (average) group delay of the channel.

Sample Clock Frequency Offset

Until now, it was assumed that the sampling clocks at the transmitter and receiver sides were frequency aligned ($f_s = \hat{f}_s$). Usually, the sample clocks are derived from a locally generated clock, and there exists a nonzero sampling frequency offset. As a result, the distance between the real epoch and the desired epoch is not constant but increases linearly with time. To reflect this time dependence, the timing error for the nth sample of the mth symbol and its estimate will be expressed as D_m^n and $\hat{D}_m^n$, respectively. The presence of the frequency mismatch results in a distortion of the FFT outputs [12, 13]. First, the useful signal component is rotated and attenuated. The angle over which the QAM symbol is rotated

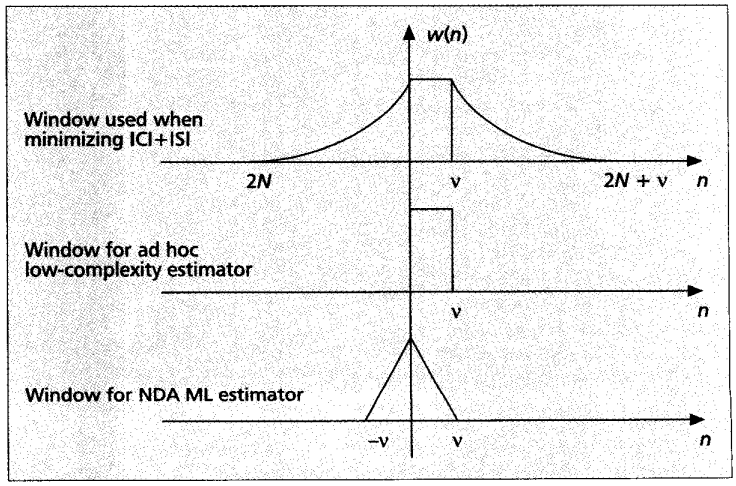

■ **Figure 6.** *Window* w(n).

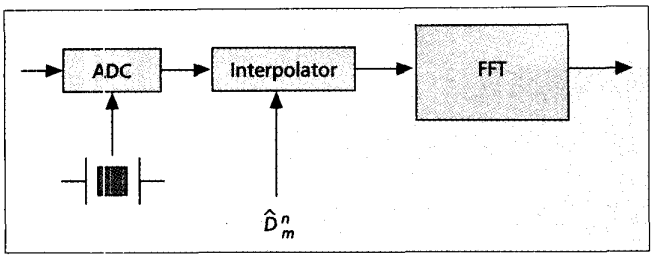

■ **Figure 7.** *An interpolator.*

is proportional to the tone index k, and increases linearly for successive DMT symbols. In addition, ICI is generated. The ICI power is proportional to the square of the carrier index and the square of the frequency offset normalized to the DMT symbol rate. Obviously, DMT systems with longer DMT symbols are more sensitive to a carrier offset. Because of the presence of a guardband, no ISI is generated. Finally, the transmitter and receiver symbol clocks desynchronize: the receiver incorrectly computes the DMT symbol period as $(2N + \nu)$ receiver sample periods.

To avoid these impairments, the receiver must estimate the timing errors. The feedback synchronizer (Fig. 2) tracks the sample clock frequency offset by feeding the filtered timing error to the TEC.

DA-ML-Based Sample Timing Estimation

After timing acquisition, the residual timing error $(D - \hat{D})$ is very small (typically a fraction of a sample period). This is reflected in a rotation of the FFT outputs. While the timing error is small decisions will be reliable, and a decision-directed timing estimation is preferred. The decisions, together with the FEQ outputs, can be used to estimate the timing error. The ML estimator computes

$$\Im\left(\sum_k \mathrm{FEQ}_m^k a_m^{*k} k \mathrm{SNR}_k\right) \quad (1)$$

It can easily be shown that linearization of this expression yields a result proportional to the timing error. Because of the presence of additive noise during transmission, this estimate is imperfect. The random variable is unbiased but gives a nonzero timing error variance. It can easily be shown that the variance of the linearized timing error is close to the Cramer-Rao bound, a fundamental lower bound on the root mean square (rms) jitter of the estimated parameter.

It is common to use only a limited set of carriers from which the timing error estimate is computed. The carriers with the largest $k^2 \times \mathrm{SNR}_k$ value produce the most accurate estimate. A measure for the signal-to-noise ratio (SNR) is known to the receiver since it has been computed during the initialization to determine the QAM constellation size for each carrier. For transmission over a far-end crosstalk (FEXT) limited channel, $k^2 \times \mathrm{SNR}_k$ is independent of k, and the timing error variance becomes inversely proportional to the number of carriers used for the estimate.

In the presence of a clock frequency offset, the timing error is time-varying from sample to sample, and the output of the timing error estimator is not exactly as in Eq. 1. In fact, ICI is added to the estimator output, which must be taken into account as self-noise when assessing the performance of the synchronizer circuit. Simulations show that for the carrier offset range of interest, degradation caused by the self-noise is tolerable.

Note that the TED produces estimates $\hat{e}_m$ on a symbol-by-symbol basis. From consecutive estimates, the frequency offset, $\Delta\hat{f}_m$, can be computed. Assuming that $\Delta\hat{f}_m$ varies only very slowly due to climatic changes, the estimates for the timing errors for each timing instant $\hat{e}_m^n$ can be computed.

Single Pilot Synchronization

In the ADSL standard [7], a single unmodulated carrier has been reserved for timing extraction. The frequency of this carrier (called the *pilot*) is fixed. Synchronization by means of a pilot has several disadvantages. Because the timing estimator exploits only a fraction of the received signal power, the variance of the timing error estimate is larger than the variance obtained when taking the multicarrier DA-ML approach. To achieve the same error variance, the closed loop bandwidth of the feedback synchronizer must be decreased. As a result, the capability of the synchronizer to track frequency offset variations is affected. Frequency offset variations can be caused by temperature changes at either side. When using an unmodulated tone, the timing error estimate becomes sensitive to a systematic, non-time-varying disturbance added to the DMT signal. Finally, if the SNR at the pilot frequency happens to be low (e.g., because of the presence of a bridged tap in the loop), the estimator produces unreliable timing estimates.

Continuous-Time Sample Timing Correction

In synchronized sampling systems, the lowpass-filtered timing error is fed back to a VCXO which is used to control the sampling device. Because of its relatively high cost, the use of a VCXO as a discrete component is to be avoided. In addition, the noise jitter on the VCXO output is usually higher than the jitter of a crystal oscillator (XO). In nonsynchronized sampling systems, the sample instants at the receiver are determined by a free-running oscillator. Timing correction is done by digital processing of the sample sequence.

Discrete-Time Domain Correction

Many methods have been developed [14] to realize a fractional delay in the discrete time domain. Usually, the timing correction is performed by means of a finite impulse response (FIR) interpolation filter (Fig. 7). The coefficients of the filter depend on the timing error to correct. Typically, for delays close to half a sample period, the filter attenuates spectral components that are close to the Nyquist frequency $\hat{f}_s/2$. This will cause a performance degradation for the highest DMT carriers. In fact, due to the time-varying filter, FFT outputs will exhibit a time-varying rotation and attenuation. This behavior is periodic with the frequency offset and should be taken into account as additional noise. This noise can be reduced to an acceptable level by oversampling the received signal $r(t)$, or by using higher-order interpolator filters (i.e., using FIR filters with a large number of coefficients). For ADSL, this method turns out to be applicable. For very-high-rate systems, such as VDSL, this approach cannot be used because of the high sampling rate and computation complexity involved. In VDSL, however, one can use synchronizer cir-

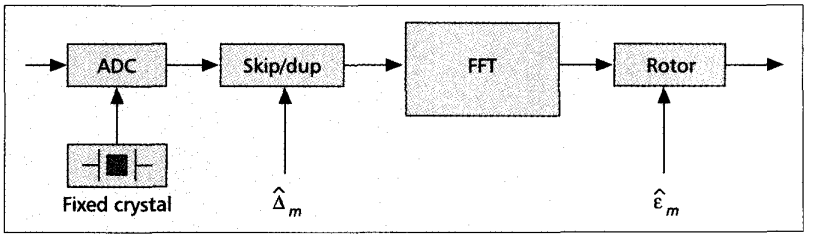

■ **Figure 8.** *Frequency domain correction.*

cuits that exploit the *delay-rotor* property.

Frequency Domain Correction

For a nonzero sample clock frequency offset, D_m^n increases linearly with time. The TED produces an output proportional to the timing errors averaged over the DMT symbol period; that is,

$$\hat{e}_m = \frac{1}{2N}\sum_{n=0}^{2N-1} e_m^n$$

Whereas ideally the timing error correction should be different for each sample, the TEC will correct the timing for each sample over the same delay. Because of the delay-rotor property, this timing correction can be performed in the frequency domain by rotating the FFT outputs (Fig. 8). A merit of this method is its low complexity. No oversampling at the receiver input is required, and for each carrier correction is performed by a single complex multiplication. Obviously, since the method is based on the (incorrect) assumption that the timing error is the same for all samples in the same DMT symbol, ICI cannot be avoided. Consequently, this method works well only when a small frequency offset can be guaranteed. This mandates very accurate (and hence more expensive) XOs at both transmitter and receiver sides. Alternatively, a low-cost, less accurate VCXO can be used to reduce the initial sample clock frequency offset. Correction of the residual offset is then performed in the digital domain.

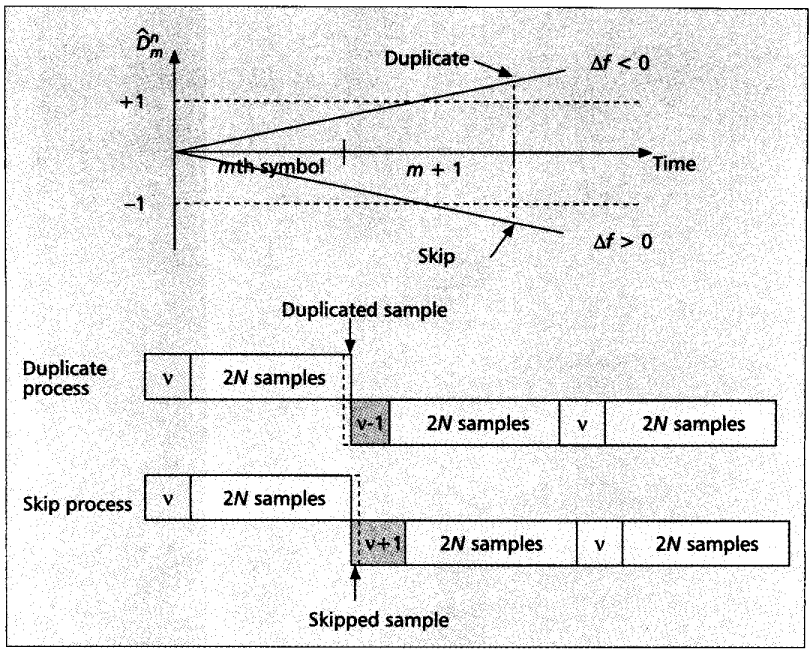

■ **Figure 9.** *Skip and duplicate.*

Symbol Synchronization In All-Digital Modems

Figure 9 depicts the increase of $\hat{D}_m^n$ as a function of time for a positive and negative sample clock frequency offset $\Delta f(\Delta f = \hat{f}_s - f_s)$. Because of the frequency mismatch, the symbol period at the receiver measured as $2N + v$ sample periods with duration $\hat{f}_s^{-1}$ ($\hat{f}_s^{-1} = (f_s + \Delta f)^{-1} = T + \Delta T$) is either too long or too short ($\Delta f < 0$, $\Delta f > 0$). Essentially, symbol clock synchronization is guaranteed by periodically shortening or enlarging the symbol period with one sample. This operation is triggered by the output of the TED, $\hat{D}_m^n$: when $\hat{D}_m$ crosses a unit boundary, the guardband is either shortened by one sample if $\hat{\Delta}_m - \hat{\Delta}_{m-1} = +1$ or enlarged by one sample if $\hat{\Delta}_m - \hat{\Delta}_{m-1} = -1$, where $\hat{\Delta}_m$ is the integer part of $\hat{D}_m$. The fractional part of $\hat{D}_m$, $\hat{\varepsilon}_m$, is corrected by the sample correction unit.

To illustrate this method, consider the DMT system based on an eight-point FFT and a guardband of five samples (Figs. 1 and 3). Assume a normalized clock frequency offset equal to 0.01 (i.e., $\Delta f/f_s = 0.01$) and that the first sample of the first symbol ($m = 0$, $n = -5$) is synchronized (i.e., $D_0^{-5} = 0$). Then the sample clock offset, D_m^n, equals $((n + 5) + (8 + 5) \times m) \times 0.01$. Obviously, the delay increases linearly. Using the delay-rotor property, a timing correction can be done for the symbol (Fig. 8). The correction is constant (i.e., the same for each sample in the symbol). The correction is computed by the TED and equals the mean delay of the samples sent to the FFT (i.e., $\hat{D}_0 = 0.085$). As a result, each sample of the symbol has a nonzero error. For example, the residual error on the first sample fed to the FFT equals $e_0^0 = 0.05 - 0.085 = -0.035$. These errors create ICI. The same process is repeated until the delay to correct exceeds the value 1. This appears for the first time with the seventh symbol as the mean delay equals $1.005T$. In this case, the correction is done in two steps. First, the timing is corrected by one sample. This is done by decreasing the length of the guardband by one sample. Second, the timing is delayed by $0.005T$ with the rotor.

Hybrid Time Domain/Frequency Domain Correction

To avoid ICI and to allow the use of inexpensive, inaccurate crystals, hybrid time/frequency domain correction can be applied (Fig. 10). This concept is shown in Fig. 11. The skip and duplicate algorithm ensures that a block of $2N$ samples is well aligned within the DMT symbol period. The sample errors, $e_m^n T$, $n \in [0, 2N - 1]$ differ only for a small amount. Indeed, when $e_m^0 T$ is the error of the first sample, the error of the nth sample can be written as $e_m^0 T + n\Delta T$.

An interpolator filter is used to correct the error increments ΔT. The values for which the FIR has to correct are minimized as follows. The timing error for the center sample in the block is not corrected. Samples to the left (right) are corrected over the values $-n\Delta T$, $n \in [1, N/2]$ ($n\Delta T$, $n \in [1, N/2)$), respectively. The corrected time epochs still have a common residual timing error bias which is eliminated by the frequency domain rotor (delay-rotor property). The main advantage of this method is that the interpolator has to correct only for small timing errors. For example, for $\Delta f/f_s = 100$ ppm and $N = 256$, the interpolator has to cor-

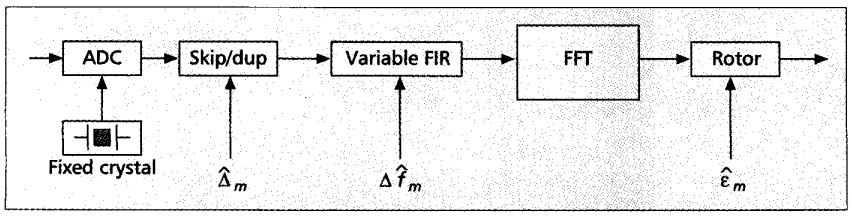

■ **Figure 10.** *Correction based on a rotor and digital interpolator.*

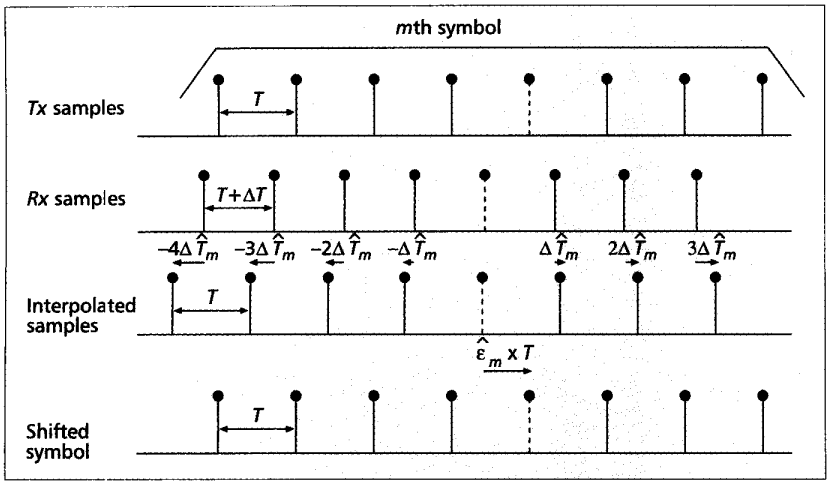

■ **Figure 11.** *Hybrid time domain/frequency domain correction.*

rect a maximal timing of 2.56×10^{-2} samples. This interpolator can be designed using a Farrow structure with only five time-invariant taps (oversampling with a factor of 2 has been assumed). The interpolator has a complexity of only a single real multiplication per sample.

A disadvantage of the presented technique is that it exploits the delay-rotor property, which is only valid under specific conditions. In reality, these conditions are not exactly met, resulting in a residual slowly time-varying ICI/ISI.

Application to Other Multi-Carrier Systems

In this article synchronization structures for transmission over static channels have been presented. Some of the concepts can be reused for transmission over time-variant channels. Applications for satellite or terrestrial transmission (i.e., digital audio broadcast and digital terrestrial television broadcast) use a simplified version of DMT called orthogonal frequency-division multiplexing (OFDM). In OFDM the constellation sizes are the same for all modulated carriers. Moreover, the complex envelope of the multicarrier signal is modulated on a separate carrier. At the receiver, IF-to-baseband conversion must be performed. This mandates estimation of additional parameters: the carrier frequency and carrier phase. If carrier frequency and phase correction are done independent of timing correction, the same estimation and correction concepts for timing synchronization can be applied.

Conclusions

In this article we focus on timing estimation and timing correction in DMT systems. NDA-ML related and ad hoc structures are presented that are suited for timing acquisition. DA-ML-based timing error estimation is considered for tracking operation. Several digital timing correction units are presented. It is shown that low-complexity circuits can be designed when the sampling clock frequency offset is corrected in the temporal domain and DMT symbol alignment is performed in the frequency domain.

Acknowledgments

The authors gratefully acknowledge the valuable comments from Peter Reusens and Raphaël Cassiers, both with Alcatel, Antwerp. The first author would like to thank Prof. M. Moeneclaey with the Communication Engineering Laboratory, University of Ghent, Belgium, for reviewing this article.

References

[1] H. L. Van Trees, *Detection, Estimation and Modulation Theory. Part 1*, New York: Wiley, 1965.

[2] L. E. Franks, "Carrier and Bit synchronization in Data Communication — A Tutorial," *IEEE Trans. Commun.*, vol. 28, no. 8, Aug. 1980, pp. 1107–20.

[3] F. M. Gardner, "Interpolation in digital modems-Part I: fundamentals," *IEEE Trans. Commun.*, vol. 41, Mar. 1993, pp. 501–7.

[4] L. Erup, F. M. Gardner, and R. Harris, "Interpolation in digital modems-Part II: Implementation and Performance," *IEEE Trans. Commun.*, vol. 44, June 1993, pp. 998–1008.

[5] H. Meyr, M. Moeneclaey, and S. A. Fechtel, *Digital Communication Receivers, Synchronization, Channel Estimation And Signal Processing*, Wiley, 1998.

[6] E. Panayirci and E. Y. Bar-Ness, "A New Approach for Evaluating the Performance of a Symbol Timing Recovery System Employing a General Type of Nonlinearity," *IEEE Trans. Commun.*, vol. 44, no. 1, Jan. 1996.

[7] ANSI, "Network and Customer Installation Interfaces, Asymmetric Digital Subscriber Line (ADSL), Metallic Interface," T1.413-1998, 1998.

[8] J. Bingham, "Multicarrier Modulation for Data Transmission: An Idea Whose Time Has Come," *IEEE Commun. Mag.*, vol. 28, no. 5, May 1990, pp. 5–14.

[9] T. Pollet and M. Peeters, "Performance Degradation of Multi-Carrier Systems Caused by an Insufficient Guard Interval Duration," *Proc. CWAS '97*, Budapest, Oct. 27–29, 1997, pp. 125–27.

[10] J.-J. van de Beek, M. Sandell, and P. O. Borjesson, "ML Estimation of Time and Frequency Offset in OFDM systems," *IEEE Trans. Sig. Processing*, vol. 45, no. 7, July 1997, pp. 1800–5.

[11] N. Al-Dhahir and J. M. Cioffi, "Optimum Finite-Length Equalization for Multicarrier Transceivers," *IEEE Trans. Commun.*, vol. 44, no. 1, Jan. 1996, pp. 56–64.

[12] T. Pollet, P. Spruyt, and M. Moeneclaey, "The BER Performance of OFDM Systems using Non-Synchronized Sampling," *Proc. GLOBECOM '94*, San Francisco, CA, Dec. 27–29, 1994, pp. 253–57.

[13] T. N. Zogakis and J. M. Cioffi, "The Effect of Timing Jitter on the Performance of a Discrete Multitone Signal," *IEEE Trans. Commun.*, vol. 44, July 1996, pp. 799–808.

[14]T. Laakso *et al.*, "Splitting the Unit Delay: Tools for fractional delay filter design," *IEEE Sig. Processing*, Jan. 1996, pp. 30–60.

Biographies

THIERRY POLLET (Thierry.Pollet@alcatel.be) received a Diploma degree in electrical engineering from the University of Ghent in 1989. From 1989 to 1996 he was employed at the Communications Engineering Laboratory, University of Ghent, as a research assistant. In 1996 he joined the Corporate Research Center of Alcatel, Antwerp, Belgium. Currently, he is in charge of xDSL transmission developments in the research department. His main research interests are high-speed copper transmission, digital communications, equalization, and synchronization.

MIGUEL PEETERS received an M.S. degree in electrical engineering from Free University of Brussels, Belgium, and Ecole Centrale Paris, France, in 1996. His thesis was about the shaping of light impulses for gigabit solution transmission. In September 1996 he joined the Alcatel Corporate Research Center in Antwerp, Belgium, where he is currently a research engineer. His current research topics cover synchronization, equalization, and design of multicarrier systems for xDSL transmission.